

• Supplementary File •

# Beam Alignment for Millimeter Wave Multiuser MIMO Systems Using Sparse-Graph Codes

Long CHENG<sup>1</sup>, Guangrong YUE<sup>1\*</sup>, Pei XIAO<sup>2</sup>, Ning WEI<sup>3,4</sup> & Shaoqian Li<sup>1</sup>

<sup>1</sup>*National Key Laboratory of Science and Technology on Communications,  
University of Electronic Science and Technology of China, Chengdu 611731, China;*

<sup>2</sup>*5GIC & 6GIC, Institute for Communication Systems (ICS),  
University of Surrey, United Kingdom.;*

<sup>3</sup>*ZTE Corporation, Shenzhen 518057, China;*

<sup>4</sup>*State Key Laboratory of Mobile Network and Mobile Multimedia Technology, Shenzhen 518055, China*

## Appendix A Three Classifications of Observation Nodes

According to the distribution of multipath direction of mmWave channel, we can classify the observation detections based on its edge degree as follows:

1. **zero-ton:** A right node is a zero-ton if it is not connected to any non-zero entry of the angle domain channel  $\hat{\mathbf{h}}_k$ .
2. **single-ton:** A right node is a single-ton if it is connected to only one non-zero entry of the angle domain channel  $\hat{\mathbf{h}}_k$ .
3. **multi-ton:** A right node is a multi-ton if it is connected to more than one non-zero entry of the angle domain channel  $\hat{\mathbf{h}}_k$ .

## Appendix B The Minimum Threshold Value of $\eta$ of the Number of Stage $d$

**Table B1** The Minimum Threshold Value of  $\eta$  of the Number of Stage  $d$

d	3	4	5	6	7	8
$\mu$	0.407	0.323	0.285	0.261	0.245	0.233
$d\mu$	1.221	1.292	1.425	1.566	1.715	1.864

## Appendix C Proof of Theorem 1

Define  $Y$  as the total number of edges that are not decoded over a random graph from the ensemble  $\mathfrak{R}^K(F, m)$ , we have

$$\begin{aligned} \mathbb{E}(Y) &< 2Kdp_i, \\ P(|Y - \mathbb{E}(Y)| > Kd\varsigma) &< e^{-\delta\varsigma^2 K^{1/(4i+1)}}, \end{aligned} \quad (C1)$$

where  $\delta, \varsigma$  denote the variable parameters,  $\varsigma$  is the arbitrary parameter, and  $p_i$  is the probability of the event that an edge exists after the  $i$ -th peeling off operation.

Furthermore, to derive the expression of  $p_i$ , we define the edge degree distribution in the ensemble as

$$\begin{aligned} \lambda(\alpha) &= \sum_{i=1}^{\infty} \lambda_i \alpha^{i-1}, \\ \rho(\alpha) &= \sum_{i=1}^{\infty} \rho_i \alpha^{i-1}, \end{aligned} \quad (C2)$$

where  $\lambda_i$  and  $\rho_i$  are the probability that the edge connected to the left (resp. right) node with degree  $i$ . For the proposed *beam-and-detection* procedure,  $\lambda(\alpha) = \alpha^{d-1}$ . Furthermore, considering that the degree of a right node follows the binomial distribution  $B(1/\eta K, K)$ , we have

$$\begin{aligned} \rho_i &= i\eta P(\text{a right node has edge degree } i), \\ &\approx \frac{(1/\eta)^{i-1} e^{-1/\eta}}{(i-1)!}. \end{aligned} \quad (C3)$$

Thus, the edge degree distribution polynomial  $\rho(\alpha)$  is given by

$$\rho(\alpha) = e^{-(1-\alpha)/\eta}, \quad (C4)$$

---

\* Corresponding author (email: yuegr@uestc.edu.cn)

Then, under the cycle-free assumption, the probability  $p_i$  in (C1) for the ensemble  $\mathfrak{R}^K(F, m)$  can be expressed as

$$p_{i+1} = (1 - e^{-\frac{p_i}{\eta}})^{d-1}, \quad (\text{C5})$$

where  $p_1=1$ , and the choice of  $\eta$  is given to guarantee  $p_{i+1} < p_i$  e.g., see Table B1.

According to Eq. (C1), we can draw the conclusion that with high probability, the proposed peeling off decoder captures all but a small fraction of the variable nodes. However, in a real application scenario, we need to ensure all the variable nodes to be recovered. Therefore, based on the above conclusions, we next study how to complete all the decoding work.

Without loss of generality, in this appendix, we consider a set of left non-zero nodes  $P$  in the random graph  $\mathfrak{R}^K(F, m)$ , and the corresponding right neighborhood  $N_i(P)$  of the  $i$ -th subset of the right nodes. Note that the proposed peeling off decoder fails when there are no single-ton nodes in the  $N_i(P)$  for  $i = 1, \dots, d$ . Further, a sufficient condition for the above hypothesis is that the average degree of all the nodes in the neighborhood of  $P$  (i.e.  $|N_i(P)|$  for all the  $i$ ) is less than 2, such as  $|N_i(P)| > |P|/2$ . Specifically, if the average degree of the right nodes is less than 2, the single-ton must occur. Then, considering that  $f_i = \eta K + O(1)$ , we will discuss the probability of the opposite event  $\mathfrak{S}$ , i.e.,  $\max\{|N_i(P)|\}_{i=1}^d \leq |P|/2$  as follows:

$$\begin{aligned} \Pr(\mathfrak{S}) &< \prod_{i=1}^d \left( \frac{|P|}{2f_i} \right)^{|P|} \left( \frac{f_i}{|P|/2} \right) \\ &\approx \left( \frac{|P|}{2\eta K} \right) \left( \frac{\eta K}{|P|/2} \right)^d \\ &< \left( \frac{|P|}{2\eta K} \right) \left( \frac{2\eta K e}{|P|} \right)^{d|P|/2} \\ &= \left( \frac{|P| e}{2\eta K} \right)^{d|P|/2}. \end{aligned} \quad (\text{C6})$$

Further, by using a union bound, the probability of event  $\mathfrak{N}_s$  that there exist some sets of the variable nodes that follow the rules, i.e.,  $\max\{|N_i(P)|\}_{i=1}^d \leq |P|/2$ , we have

$$\begin{aligned} \Pr(\mathfrak{N}_s) &< \Pr(\mathfrak{S}) \left( \frac{K}{|P|} \right) \\ &< \left( \frac{|P| e}{2\eta K} \right)^{d|P|/2} \left( \frac{K e}{|P|} \right)^{|P|} \\ &< \left[ \left( \frac{|P|}{\eta K} \right)^{d-2} \left( \frac{e}{2} \right)^d \left( \frac{e}{\eta} \right)^2 \right]^{|P|/2} \\ &\stackrel{(a)}{<} O\left( (|P|/m)^{|P|/2} \right) \end{aligned} \quad (\text{C7})$$

where (a) comes from the fact that  $d \geq 3$  and  $m = O(\eta K)$ . Then, according to  $|P| = O(K)$ , we get

$$\Pr(\mathfrak{N}_s) < O(1/m), \quad (\text{C8})$$

Finally, based on Eq. (C1), Eq. (C5) and Eq. (C8), **Theorem 1** can be proved.

## Appendix D Proposed Noiseless Beam Alignment Algorithm

In this appendix, a noiseless beam alignment algorithm is proposed for mmWave MU-MIMO systems. Considering that in the noiseless case, the mmWave uplink multi-user channel only retains  $K$  LOS paths, then we design the bin detection matrix  $\mathbf{S}$  as follows:

$$\mathbf{S} = \begin{bmatrix} 1 & 1 & \dots & 1 \\ 1 & e^{j\frac{2\pi}{KM_T}} & \dots & e^{j\frac{2\pi}{KM_T}(KM_T-1)} \end{bmatrix}. \quad (\text{D1})$$

Therefore, the  $b$ -th left node is modulated by the  $b$  column of the matrix  $\mathbf{S}$ . Furthermore, each right node is connected to a bin measurement vector  $\mathbf{r}^b = [r^b[1], r^b[2]]^T$ . Then, in order to effectively identify whether each measured right node is a zero-ton, single-ton or multi-ton, we design the identification method as follows

1. **zero-ton identification:** A measured right node is a zero-ton if all the measurements are zero, such as

$$r^i[1]=r^i[2]=0. \quad (\text{D2})$$

2. **single-ton identification:** The single-ton identification is utilized to obtain the index of the estimated beam and the magnitude as follows:

$$\begin{aligned} \tilde{b} &= \frac{\angle r^i[2]/r^i[1]}{2\pi/KM_T}, \\ \tilde{\mathbf{h}}[\tilde{b}] &= r^i[1], \end{aligned} \quad (\text{D3})$$

where the measured node can be judged as a single-ton only if the estimated index  $\tilde{b}$  is an integer.

3. **multi-ton identification:** A measured right node is a multi-ton if the measured vector complies with the following rules

$$\begin{aligned} \tilde{i} &= \frac{\angle r^i[2]/r^i[1]}{2\pi/KM_T} \neq \text{integer}, \\ |r^i[2]| &\neq |r^i[1]|. \end{aligned} \quad (\text{D4})$$

Finally, combined with the *peeling off* method, the proposed noiseless beam alignment algorithm is proposed. And then, the detail steps are listed in the Algorithm D1.

**Algorithm D1** Noiseless Beam Alignment Algorithm Using Sparse-Graph Codes

**Require:** Received signal  $\mathbf{r}$ , measurement matrix  $\boldsymbol{\psi}$ , sparse coding matrix  $\mathbf{G}$  and bin detection matrix  $\mathbf{S}$ , number of users  $K$  and number of iterations  $L$ .

**Ensure:** The estimated index of beam channel  $\tilde{b}$  and magnitude  $\tilde{\mathbf{h}}$ .

```

for iteration  $1 < l < L$  do
  for stage  $1 < i < d$  do
    for bin  $1 < j < f_i$  do
      if  $\|\mathbf{r}_{i,j}[1]\| = 0$  then
         $\mathbf{r}_{i,j}$  is a zero-ton bin vector.
      else
        identify if  $\mathbf{r}_{i,j}$  is a single-ton bin vector and get the estimated index-value pair  $\langle \tilde{b}, \tilde{\mathbf{h}}[\tilde{b}] \rangle$ .
        if single-ton = 'true' then
          peeling off:  $\mathbf{r}^{l+1} = \mathbf{r}^l - \tilde{\mathbf{h}}[\tilde{b}] \begin{pmatrix} 1 \\ e^{j \frac{2\pi \tilde{b}}{KM_T}} \end{pmatrix}$ 
        else
          bin vector  $\mathbf{r}_{i,j}$  is a multi-ton bin vector.
        end if
      end if
    end for
  end for
end for
end for

```

$$\begin{array}{ccc}
 \begin{bmatrix} 1 & 0 & 0 & 1 & 0 & 0 \\ 0 & 1 & 0 & 0 & 1 & 0 \\ 0 & 0 & 1 & 0 & 0 & 1 \\ 1 & 0 & 1 & 0 & 1 & 0 \\ 0 & 1 & 0 & 1 & 0 & 1 \\ 0 & 1 & 0 & 1 & 0 & 1 \\ 1 & 0 & 1 & 0 & 1 & 0 \end{bmatrix} & \Rightarrow & \begin{bmatrix} \mathbf{D}_1[1] & 0 & 0 & \mathbf{D}_1[2] & 0 & 0 \\ 0 & \mathbf{D}_1[1] & 0 & 0 & \mathbf{D}_1[2] & 0 \\ 0 & 0 & \mathbf{D}_1[1] & 0 & 0 & \mathbf{D}_1[2] \\ \mathbf{D}_2[1] & 0 & \mathbf{D}_2[2] & 0 & \mathbf{D}_2[3] & 0 \\ 0 & \mathbf{D}_2[1] & 0 & \mathbf{D}_2[2] & 0 & \mathbf{D}_2[3] \\ 0 & \mathbf{D}_3[1] & 0 & \mathbf{D}_3[2] & 0 & \mathbf{D}_3[3] \\ \mathbf{D}_3[1] & 0 & \mathbf{D}_3[2] & 0 & \mathbf{D}_3[3] & 0 \end{bmatrix} \\
 \mathbf{G} & & \boldsymbol{\psi}
 \end{array}$$

**Figure E1** An illustration of the sparse codes with its associated measurement matrix, while the coding matrix has three stages with  $f_1 = 3$ ,  $f_2 = 2$  and  $f_3 = 2$ . Note that  $\mathbf{D}_i[x]$  denotes the  $x$ -th column of the bin matrix  $\mathbf{D}_i$ .

## Appendix E Proposed Robust Beam Alignment Algorithm Using Sparse-Graph Codes

In this appendix, a robust beam alignment algorithm is proposed to enhance robustness in noisy environments. In a real multi-user scenario, we only need to acquire the LOS path for each user [1]. Then we can utilize the same regular graph  $\Gamma^{MT}(R, b)$  as mentioned in previous section to ensure the success probability of beam detection, as it provides a theoretical bound for beam scanning. However, in the noisy scenario, the data received is contaminated and cannot be simply indexed by calculation, we thus propose a new bin detection matrix  $\mathbf{D}$  in the sequel.

Since only a few beams in specific directions are sent each time for beam scanning, we can also design the bin detection matrix  $\mathbf{D}$  to be sparse, that is, the beams in different directions have different weights each time. Specifically, in each stage of the sparse coding matrix  $\mathbf{G}$ , we design the corresponding special bin matrix  $\mathbf{D}_i \in \mathbb{C}^{N \times M_i}$ , where  $M_i$  is the number of non-zero entries in each stage of the matrix  $\mathbf{G}$ . In particular, considering the presence of noise, each entry of the matrix  $\mathbf{D}_i$  is randomly selected from a unit circle [2]. Further, an example is shown in Fig. E1 to illustrate the relationship between measurement matrix  $\boldsymbol{\psi}$  and sparse coding matrix  $\mathbf{G}$ .

Based on the special structure of measurement matrix, we propose a robust detection scheme for each bin. Firstly, we simple check if the received vector is zero-ton as follows

$$\|\mathbf{r}_{i,j}[1]\| \leq (\delta_{\min}^2 \varepsilon_1 + \sigma_{\min}^2), \quad (\text{E1})$$

where  $\delta_{\min}^2$  denotes the minimum signal power,  $\sigma_{\min}^2$  is the minimum noise power, and  $\varepsilon_1$  is the **zero-ton** detection threshold. In particular, it seems that the values of the minimum signal power  $\delta_{\min}^2$  and the minimum noise power  $\sigma_{\min}^2$  influence the final decision. However, since the minimum signal power and minimum noise power have been determined as a standard when sending signals, we use tuning factor  $\varepsilon_1$  to adjust them.

we assume the received bin vector is a single-ton and then estimate the index pair  $\langle \tilde{b}, \tilde{\mathbf{h}}[\tilde{b}] \rangle$ . Specifically, for bin  $j$  of stage  $i$ , a maximum likelihood (ML) method is utilized to obtain the possible coefficient for the  $k$ -th column of the bin matrix  $\mathbf{D}_i$  as follows:

$$\alpha_k = \frac{\mathbf{D}_i^H[k] \mathbf{r}_{i,j}}{\|\mathbf{D}_i[k]\|^2}. \quad (\text{E2})$$

Then, the estimated  $\tilde{k}$  is the one which minimizes the residual, i.e.,

$$\tilde{k} = \arg \min_{1 < k < M_i} \|\mathbf{r}_{i,j} - \alpha_k \mathbf{D}_i[k]\|. \quad (\text{E3})$$

Furthermore, a *check* procedure is proposed to determine if it is a single-ton, according to the following criterion

$$\frac{1}{M_i} \|\mathbf{r}_{i,j} - \tilde{\alpha}_k \mathbf{D}_i[\tilde{k}]\| \leq (\delta_{\min}^2 \varepsilon_2 + \sigma_{\min}^2), \quad (\text{E4})$$

**Algorithm E1** Robust Beam Alignment Algorithm Using Sparse-Graph Codes

**Require:** Received signal  $\mathbf{r}$ , measurement matrix  $\boldsymbol{\psi}$ , sparse coding matrix  $\mathbf{G}$  and bin detection matrix  $\mathbf{D}_i$  for all stages, number of users  $K$ , number of iterations  $L$ , error threshold  $\varepsilon_1$ , initialization parameter  $K_{ue} = 0$  and error threshold  $\varepsilon_2$

**Ensure:** The estimated index of beam channel  $\tilde{b}$  and magnitude  $\tilde{\mathbf{h}}$ .

```

for iteration  $1 < l < L$  do
  for stage  $1 < i < d$  do
    for bin  $1 < j < f_i$  do
      if Eq. (E1) is real then
         $\mathbf{r}_{i,j}$  is a zero-ton bin vector.
      else
        for index  $1 < k < M_i$  do
          if  $K_{ue} \leq K$  then
            get the estimated index-value pair  $\langle \tilde{k}, \tilde{\alpha}_{\tilde{k}} \rangle$  by using Eq. (E2), Eq. (E3).
            identify if the received bin vector is a single-ton by using Eq. (E4).
            if single-ton = 'true' then
              obtain  $\tilde{b}$  by utilizing the estimated  $\tilde{k}$  and the coding pattern in the  $j$ -th bin of the  $i$ -th stage.
               $\tilde{\mathbf{h}}[\tilde{b}] = \tilde{\alpha}_{\tilde{k}}$ .
              peeling off:  $\mathbf{r}^{l+1} = \mathbf{r}^l - \tilde{\mathbf{h}}[\tilde{b}]\mathbf{D}_i[\tilde{k}]$ .
               $K_{ue} = K_{ue} + 1$ ;
            else
              bin vector  $\mathbf{r}_{i,j}$  is a multi-ton bin vector.
            end if
          else
            break.
          end if
        end for
      end if
    end for
  end for
end for
end for
end for

```

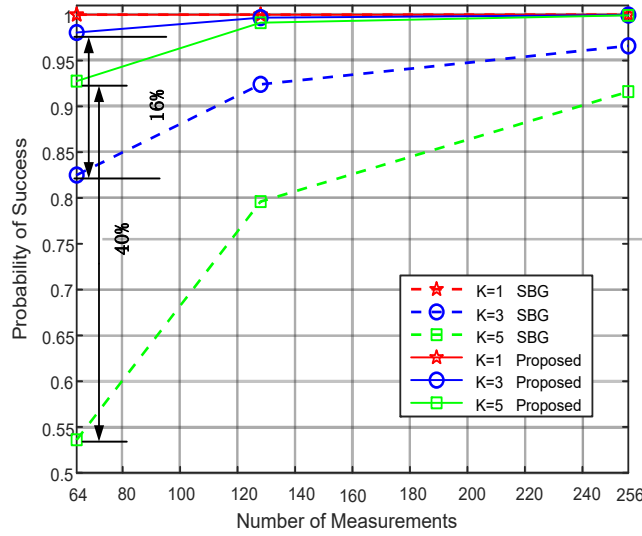


**Figure F1** Comparison of the probability of success among the proposed method and the fast beam alignment method versus different measurement cost.

where  $\delta_{\min}^2$  denotes the minimum single power,  $\sigma_{\min}^2$  is the minimum noise power, and similar to the zero-ton detection threshold  $\varepsilon_1$  in Eq. (E1),  $\varepsilon_2$  is the single-ton detection threshold.

Finally, the estimated  $\tilde{k}$  can be mapped to the real index  $\tilde{b}$  and the detailed steps are listed in the Algorithm E1.

## Appendix F Simulation Results

In this section, we consider a mmWave Massive MIMO system with hybrid precoding architecture at both the UEs and the BS. In particular, the BS utilizes a ULA with  $N_R = 64$  and  $N_{RF} = 16$  chains to support  $K \leq 16$  UEs and the UEs utilizes a ULA with  $M_T = 16$  and  $M_{RF} = 4$  chains. For the geometric mmWave channel with noise, as mentioned above, the path loss of the NLOS paths is always higher than the LOS path, thus we consider the channel of each user is a Rician fading channel, e.g.,  $L_k = 4, K_{factor} = 20$  dB for  $1 < k < K$  [1]. Then, we utilize a regular graph  $\mathfrak{R}_d^K(F, m)$  to construct the measurement matrix, where it has  $d \geq 3$  stages. In Algorithm D1 and Algorithm E1, we take  $L = 4$  to strike a better tradeoff between the performance and complexity order. In particular, for the threshold in Algorithm E1, we set  $\varepsilon_1 = 0.04$  and  $\varepsilon_2 = 0.15$ , so that the algorithm we proposed can achieve the best performance for different scenarios.

In the following simulations, we evaluate the performance of our proposed scheme according to three viewpoints: i) under the

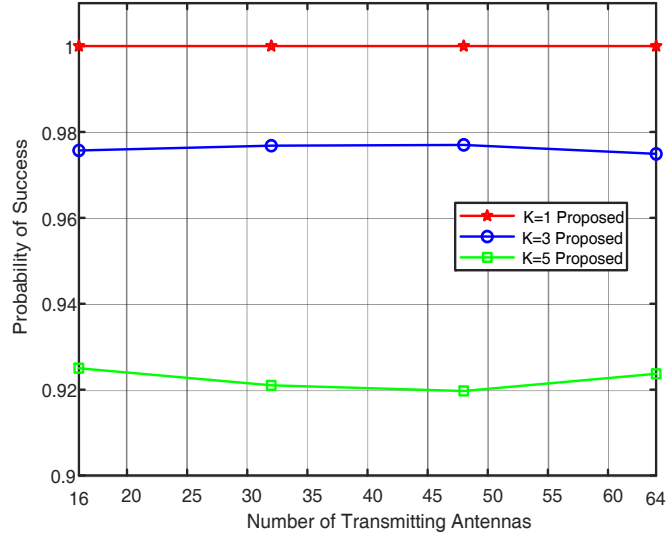


**Figure F2** Probability of success of the proposed method versus different number of transmitting antennas, where the number of measurements is 64.

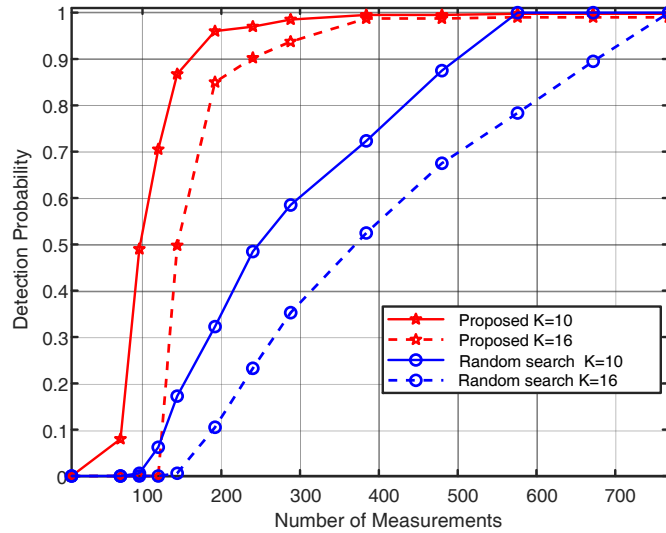


**Figure F3** Comparison of the detection probability obtained by the proposed algorithm, the random search algorithm in the case of full beam alignment as a function of measurement cost, where SNR = 5 dB, and  $N_c = 32$  in the random search algorithm.

noiseless setting, we show the superiority of our proposed noiseless beam alignment algorithm over recent proposed algorithm [3] through the probability of success, such as

$$\frac{\|\tilde{\mathbf{h}} - \hat{\mathbf{h}}\|_2^2}{\|\hat{\mathbf{h}}\|_2^2} \leq 10^{-6}, \quad (\text{F1})$$

where a trial is considered successful if the above equation is satisfied; ii) under the noise setting, we compare the detection probability of the LOS path with recent proposed random search algorithm, where a success means if the strongest component of each UE coincides with the central of the strongest scatterer cluster; iii) in order to examine the estimation performance of our algorithm, we compare it with the classical compressed sensing algorithm [1], which not only compare the measurement cost, estimation accuracy, but also includes the calculation time and complexity.

## Appendix F.1 Noiseless Case

Fig. F1 depicts the probability of success versus different number of measurements of the proposed scheme in comparison with the fast beam alignment algorithm introduced in [3]. As shown in Fig. F1, even the number of measurements is very small (32), our proposed noiseless algorithm still achieves a high probability of success (over 90%). Furthermore, compared with the beam alignment algorithm [3], our algorithm provides considerable performance gains up to 16% ( $K = 3$ ) and 40% ( $K = 5$ ) in the success rate. This benefit is due to the fact that our proposed algorithm takes advantage of the *peeling off* method and the density evolution to guarantee the bound achieving performance, even though the fast beam alignment method utilizes a similar precoding structure.

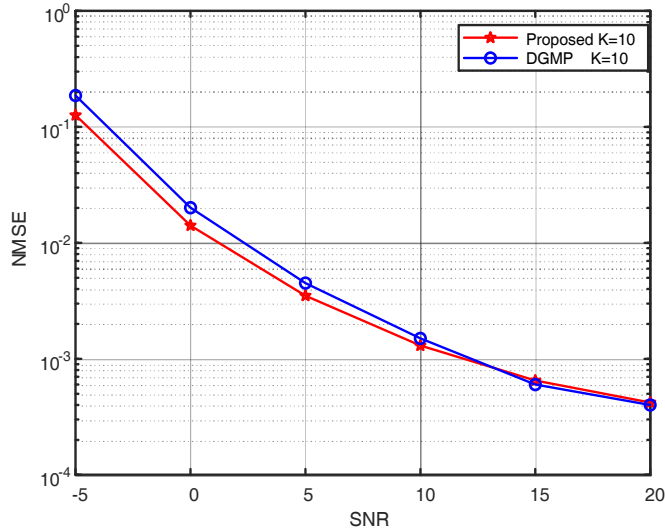


**Figure F4** Comparison of the NMSE obtained by the proposed algorithm, the DGMP algorithm as a function of SNR, where  $K = 10$ . In particular, the number of measurements for the two algorithms is 256 and 96, respectively.

**Table F1** Average Run Time of Respective Algorithms:  $K = 10$ , SNR = 20 dB

ALG	NMSE	Average Run Time(s)
DGMP	4.0013e-4	27.785
Proposed	4.2131e-4	0.565

Furthermore, in Fig. F2, the probability of success as a function of the number of transmitting antennas is presented. One can observe that the performance of our proposed scheme remains constant with the growth of  $M_T$ . This phenomenon implies that the proposed scheme has a measurement independent of  $M_T$ .

## Appendix F.2 Noise Case

To compare with the state-of-the-art beam alignment algorithm, we utilize the random search algorithm, which is modelled as a best case of [4]. Specially, at each time  $t$ , the random search algorithm randomly selects a multidirectional beamforming vector  $w_t$  and utilizes the PN sequences to ensure the orthogonality of different beams. Then, under the noise setting, the detection probability of the proposed robust beam alignment scheme is compared with the recent random search scheme for  $K = 10$  and  $K = 16$ . In particular, we define a success if the location of the strongest component of the AoAs/AoDs can be detected. As observed in Fig. F3, the proposed algorithm outperforms the random search scheme v.s. different number of measurements. The performance improvement is due to that even though the random search method also sends multiple beams, it requires a longer sequence to maintain the orthogonality of multiple beams. In particular, there is a marked improvement when the measure cost from 96 to 120. This particular phenomenon may be due to the fact that the redundancy parameter  $\mu$  for constructing this measurement exactly meets the conditions of **Theorem 1**.

Moreover, different from the conventional beam alignment algorithms such as the random search method, our proposed algorithm can extract information such as channel complex gain according to Eq. (E2), so the estimated channel can be reconstructed. Thus, in order to make a comparison with the traditional CS-based algorithm, Fig. F4 examines the performance of the proposed algorithm and the distributed grid matching pursuit (DGMP) algorithm [1] at different SNRs in the case of full beam alignment. Compared with the traditional CS-based algorithm, the proposed beam alignment algorithm can achieve the similar estimated performance at the cost of longer pilot sequences. However, as shown in Table F2, the DGMP algorithm incurs a prohibitive computational complexity due to the large matrix operation, especially the matrix inversion. Furthermore, the simulation results above show that our algorithm achieves a good trade-off between sampling complexity and computational complexity.

## References

- Gao Z, Hu C, Dai L, et al. Channel estimation for millimeter-wave massive MIMO with hybrid precoding over frequency-selective Fading Channels. *IEEE Communications Letters*, 2016, 20: 1259-1262
- Zhou Z, Fang J, Yang L, et al. Low-rank tensor decomposition-aided channel estimation for millimeter wave MIMO-OFDM systems. *IEEE Journal on Selected Areas in Communications*, 2017, 35: 1524-1538
- Li X, Fang J, Duan H, et al. Fast beam alignment for millimeter wave communications: a sparse encoding and phaseless decoding approach. *IEEE Transactions on Signal Processing*, 2019, 67: 4402-4417
- Abari O, Hassanieh H, Rodriguez M, et al. Millimeter wave communications: from point-to-point links to agile network connections. In: *Proceedings of 15th ACM Workshop Hot Topics Networks*, New York, USA, 2016, 169-175